Energy 36 (2011) 133–140

Contents lists available at ScienceDirect

Energy

journal homepage: www.elsevier.com/locate/energy

Development of an energy-saving module via combination of solar cells and thermoelectric coolers for green building applications

Tsung-Chieh Cheng [a], Chin-Hsiang Cheng [b,*], Zhu-Zin Huang [a], Guo-Chun Liao [a]

[a] Department of Mechanical Engineering, National Kaoshiung University of Applied Science, Kaoshiung City, Taiwan, ROC
[b] Department of Aeronautics and Astronautics, National Cheng Kung University, No.1, Ta-Shieh Road, Tainan 70101, Taiwan, ROC

ARTICLE INFO

Article history:
Received 19 April 2010
Received in revised form
2 October 2010
Accepted 30 October 2010
Available online 21 December 2010

Keywords:
Solar cell
Thermoelectric cooler
Regeneration water channels
Green building

ABSTRACT

A solar-driven thermoelectric cooling module with a waste heat regeneration unit designed for green building applications is investigated in this paper. The waste heat regeneration unit consisting of two parallel copper plates and a water channel with staggered fins is installed between the solar cells and the thermoelectric cooler. The useless solar energy from the solar cells and the heat dissipated from the thermoelectric cooler can both be removed by the cooling water such that the performance of the cooling module is elevated. Moreover, it makes engineering sense to take advantage of the hot water produced by the waste heat regeneration unit during the daytime. Experiments are conducted to investigate the cooling efficiency of the module. Results show that the performance of the combined module is increased by increasing the flow rate of the cooling water flowing into the heat regeneration water channel due to the reductions of the solar cell temperature and the hot side temperature of the thermoelectric coolers. The combined module is tested in the applications in a model house. It is found that the present approach is able to produce a 16.2 °C temperature difference between the ambient temperature and the air temperature in the model house.

1. Introduction

Under the inevitable influence of the energy shortage and the rise of environmental awareness, promising energy sources to satisfy the world's growing energy demand has received increasing attention in the past several decades. In recent years, energy conservation is achieved through efficient energy consuming or energy-saving methods, in which energy use is decreased while achieving a similar outcome, or by reduced consumption of energy services. For these purposes, renewable energy coming from natural resources such as sunlight, wind, tides, and geothermal heat are of great interests to the energy technology researchers. Mousazadeh et al. [1] showed that covering 0.16% of the land on earth with 10% efficient solar conversion systems would provide 20 TW of power, nearly twice the world's consumption rate of fossil energy. Therefore, solar cells are one of the promising technologies to convert the incident solar radiation into electric power by the photovoltaic (PV) effect [2]. The development of the solar cell seems from the researches of the French physicist Antoine-César Becquerel in 1839, but the first solar cell was built by American inventor Charles Fritts, who coated the selenium with thin layer of gold to form the junctions with 1% conversion efficiency. In planning for the future scaling-up photovoltaic power generation, it is essential to carefully choose the semiconductor materials. Recent development seemingly indicates that GaAs is most materials for promising PV technologies; however, since the cost of the GaAs solar cells is relatively more expensive than those made of crystalline silicon, over 80% of the world's solar cells and module productions are currently made of sliced single crystal or polycrystalline silicon cells [3]. However, a lot of issues, considering the long term stability and temperature effect on the cells, need to be clarified prior to commercial breakthrough of the technology [4]. The operating cell temperature greatly affects its efficiency through the functional dependence of the different physical parameters, such as short-circuit current, open-circuit voltage, light absorption and the fill factor, on the cell temperature [5,6]. In general, the voltage output and life expectancy of a solar cell will be decreased with increasing temperature. Therefore, controlling the operating temperature is an important factor for the solar cells [7].

Thermoelectric material can be used to directly convert heat into electricity, or vice versa. It can be used in two major operating

* Corresponding author. Tel.: +886 6 2757575x63627; fax: +886 6 2389940.
E-mail address: chcheng@mail.ncku.edu.tw (C.-H. Cheng).

0360-5442/$ – see front matter
doi:10.1016/j.energy.2010.10.061

Nomenclature

G	geometric factor
I	input current (A)
K	thermal conductivity of thermoelectric element (W/m-°C)
N	number of thermoelectric element pairs
$\boldsymbol{P}$	output power of solar cell (mW)
Q	flow rate of cooling water (ml/min)
Q_h	rate of heat dissipated from hot side of a thermoelectric cooler (W)
Q_c	rate of heat absorbed by cold side of a thermoelectric cooler (W)
T_o	ambient temperature (°C)
T_{in}	entering cooling water temperature (°C)
T_{out}	exiting cooling water temperature (°C)
T_{room}	temperature of the air in tmodel house (°C)
T_{sc}	temperature of solar cell (°C)
T_t	average temperature of cooling water in heat regeneration water channel (°C)
T_{tecc}	cold side temperature of the thermoelectric cooler (°C)
T_{tech}	hot side temperature of the thermoelectric cooler (°C)
T_∞	ambient temperature (°C)
t	time (sec)
W_{in}	power input for TEC (W)
x	measured variable
Greek symbols	
α	Seebeck coefficient (V/°C)
ΔT	temperature difference between the hot and the cold sides (°C)
ρ	electrical resistivity of thermoelectric material (Ω-m)

models: thermoelectric generator (TEG) [8] and thermoelectric cooler (TEC). Thermoelectric cooler is a solid-state active heat pump which transfers heat from the cold side of the device to the hotter side against the temperature gradient, with consumption of electricity. A numerical model for simulation of transient, three-dimensional thermal characteristics of the thermoelectric coolers was presented by Cheng et al. [9]. Different from the vapor-compression refrigeration systems, the thermoelectric cooler does not require the components like compressor, expansion valve, evaporator, condensers, or solution pumps. Moreover, it does not require working fluids or utilize any moving parts. Because of the advantages such as high reliability, flexibility in packaging and integration, and low weight, the thermoelectric coolers are regarded as clean and active cooling methods which have been widely used in military, aerospace, instrument, and industrial products. When a TEC is used for cooling purposes, the TEC must be designed based on required cooling capacity at a proper coefficient of performance (COP) [10,11]. In practices, the performance of the TECs is strongly dependent on several operating parameters, namely, the temperatures of the TEC cold and hot sides [12], thermal and electrical conductivities of TEC elements [13], thermal contact resistance between the TEC cold side and the cooled device surface, thermal resistance of the heat sink placed on the TEC hot side [14], and the applied electric current [15].

Furthermore, a number of studies have been performed to investigate the performance of the combined systems of the thermoelectric cooler and the solar cells. Hara et al. [16] installed the solar cell-driven thermoelectric coolers at the front of a headgear to cool the forehead for outside personal cooling device, and Mei et al. [17] studied a solar-assisted automobile thermoelectric air conditioner. Lately, Bansal and Martin [18] compared the relative performance among the vapor-compression refrigeration system, the solar cell-driven thermoelectric cooler, and the absorption refrigerators.

Recently, global increasing demand for air conditioning for buildings led to production of more electricity and consequently more release of CO_2 all over the world. A recent report of Xi et al. [19] indicated that the energy consumption for air-conditioning systems is estimated to 45% of the whole households and commercial buildings. It is recognized that the thermoelectric coolers and the solar cells combined system can be used for the air-conditioning applications, and the technology actually meets the demand for energy conservation and environment protection. Chein and Chen [20] presented an expression for the heat transfer rate at the hot side of a thermoelectric cooler:

$$Q_h = 2N\left[\alpha I T_{tech} + \frac{1}{2}I^2\frac{\rho}{G} - KG(T_{tech} - T_t)\right] \quad (1)$$

where N is number of thermoelectric element pairs, α is the Seebeck coefficient, I is the input current, ρ is the electrical resistivity of the thermoelectric material, G is the thermoelectric element geometric factor, K is thermoelectric element thermal conductivity, and T_t is the average temperature of cooling water in the heat regeneration water channel. In such combined modules, the heat at the hot side of the thermoelectric cooler must be readily rejected toward the surroundings to increase the performance, while the temperature of the solar cells should be maintained at a low level to yield a high photovoltaic efficiency, as described earlier.

To the authors' knowledge, so far there is no efficient existing method available that may be used to meet the two requirements with the combined module. Therefore, in this study a solar-driven thermoelectric cooling module with a waste heat regeneration unit is proposed and tested. The waste heat regeneration unit consisting of two parallel copper plates and a water channel with staggered fins is installed between the solar cells and the thermoelectric cooler. The solar cells are mounted on the surface of one of the copper plates and the thermoelectric cooler is placed on the surface of another copper plate. The solar cells are used to provide the electricity for the thermoelectric cooler which is employed to absorb heat from the indoor space of the green building and then dissipated heat to the cooling water flowing in the regeneration channel. In this manner, the useless solar energy from the solar cells and the heat dissipated from the thermoelectric cooler can both be removed by the cooling water such that the solar cells are cooled to improve the photovoltaic efficiency and on the other hand the performance of the thermoelectric cooler is elevated because it also reduces the hot side temperature of the thermoelectric cooler. Moreover, it makes engineering sense to take advantage of the hot water, produced by the waste heat regeneration unit, for further application during the daytime. In this study, a model house with the combined module has been built for testing the feasibility of this approach, and the experimental results are provided in the following sections.

2. Experiments

2.1. Description of experimental apparatus

The tested combined module is divided into four major components: namely, solar cells, thermoelectric cooler, waste heat

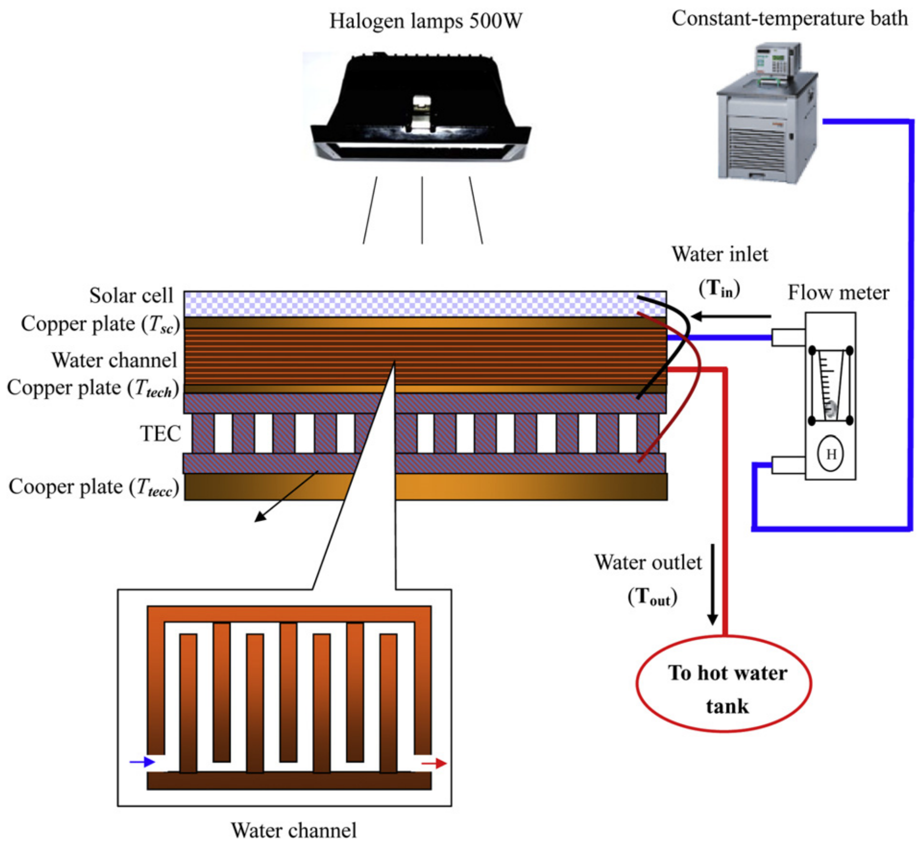

Fig. 1. Schematic diagram of the experimental system.

regeneration unit, and the measurement system, which are shown in Fig. 1. One piece of silicon crystal solar cell wafer (0.4 A × 0.5 V), which is 120 mm × 120 mm in size and 24 g in mass, is packaged on the surface of a copper plate of the heat regeneration unit by a thermal paste. The solar cell is covered by a transparent plastic film on the side facing the sun to avoid the environmental damage caused by dust in the air. Mounted on another copper plate of the heat regeneration unit are the hot sides of two 30 mm × 30 mm thermoelectric coolers. The cold sides of the thermoelectric coolers are used to cool the indoor space of the model house. In practices, a storage battery is usually employed to store the unused electricity produced during the daytime and then can be used to supply electricity for driving the thermoelectric coolers during the night time or cloudy days. However, in the present experiments, in order to fairly assess the performance of the combined module and to prevent the undesired input of the residual battery electricity to the TEC, the solar cell is directly connected to the thermoelectric coolers so as to ensure that all the electricity to the TEC is provided by the solar cell.

The heat regeneration channel made of copper has a cross-sectional area of 5 mm × 5 mm. A number of staggered fins are placed on the walls of the channel to increase the heat transfer area. The cooling water is heated by the waste heat from the solar cell and the hot sides of the thermoelectric coolers so that the water temperature is increased through the channel. The inlet cooling water temperature is fixed at 24 °C by using a constant-temperature bath. It is important to note that both the temperature of the hot side of the thermoelectric coolers and the cooling water temperature are varied with the streamwise position. In the experiments, the hot side temperature of the thermoelectric coolers (T_{tech}) is measured by averaging the temperatures detected by five T-type thermocouples installed at selected streamwise positions in between the hot side of the thermoelectric coolers and the copper plate of the channel. In addition, five more thermocouples are used to measure the cold side temperature (T_{tecc}). Similarly, the temperature of the solar cell (T_{sc}) is determined by averaging the temperature readings of the other five T-type thermocouples installed in between the solar cell and another copper plate. In addition, the packaged solar cells are exposed to a 500 W halogen lamp to simulate the stable solar light, and the distance between the halogen lamp and the solar cell is fixed at 0.5 m. Moreover, in order to measure the output power for the solar cell, a data logger (Yokogawa MV100) with a sensitivity of 0.01 mV in voltage and 0.01 A in current is used to record data of voltage and current. These data are then transferred to a PC and processed by a program developed for determination of the output power.

2.2. Uncertainty analysis

An uncertainty analysis has been carried out and the results are summarized in Table 1. Uncertainty may be caused by many sources. In this study, these sources are basically divided into four categories: environment-control uncertainty, calibration uncertainty, measurement uncertainty, and data acquisition uncertainty. The uncertainty interval for each measured variable is estimated with a 95 percent confidence using the concepts proposed by Kline and McClintock [21] and Moffat [22]. It is observed in Table 1 that the flow rate of the cooling water and the current contribute by far the largest relative uncertainty in the entire experiment. For the flow rate ranging from 1000 to 2500 ml/min, the relative uncertainty of the flow rate measurement reaches a maximum 5 percent; however, only 1 percent is found for the flow rate less than 1000 ml/min. The relative uncertainty of the flow rate measurement is mainly caused by the uncertainties of the flow rate control

Table 1
Uncertainty analysis for measured variables.

Variable	Typical value x	Uncertainty[a] δx	Relative uncertainty δx/x
Q	200–1000 ml/min	2 ml/min	1%
	1000–2500 ml/min	5 ml/min	5%
$\boldsymbol{P}$	15–40 mW	0.1 mW	0.7%
T_{sc}	24–65 °C	0.2 °C	0.8%
T_{out}, T_t	24–28	0.2 °C	0.8%
T_{tecc}	10–34 °C	0.2 °C	2%
T_{tech}	24–45 °C	0.2 °C	0.8%
T_{room}	24–36 °C	0.2 °C	0.8%
T_{∞}	24–36 °C	0.2 °C	0.8%
I	0.2–2 A	0.01 A	5%

[a] All values are estimated with 95 percent confidence.

and the accuracy of the flow meter. In addition, the relative uncertainty of current measurement is also approximately 5 percent for full range in this study. This value is partially contributed by the uncertainty of the power controller that is installed to control the input current of thermoelectric coolers from the solar cells in the model house experiments, which will be illustrated later in the subsequent section. The values listed in Table 1 involve all significant uncertainty sources and may be treated as the safest estimation of the uncertainty.

3. Experimental results and discussion

3.1. Transient/steady-state behavior of the combined module

Fig. 2 showed the results of T_{tech}, T_{tecc} and T_{sc} in a typical transient test for the solar-driven thermoelectric cooling module without cooling water flowing through the heat regeneration water channel. In this case, since the flow rate of the cooling water is set to be zero, all temperatures at different locations in this combined module increase with time monotonically. The temperature of solar cell is elevated to be 60.5 °C in 7.8 min. On the other hand, it is found that the thermoelectric coolers function well so that the

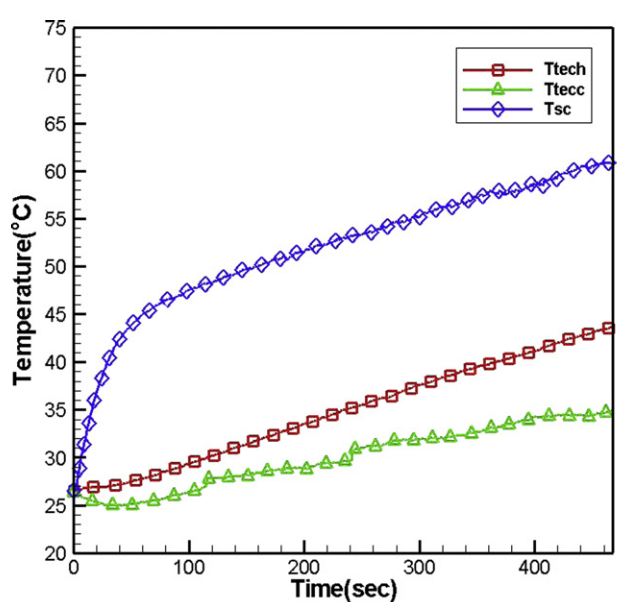

Fig. 2. Transient variation in the temperatures of solar cell and thermoelectric coolers with no cooling water flowing through heat regeneration water channel.

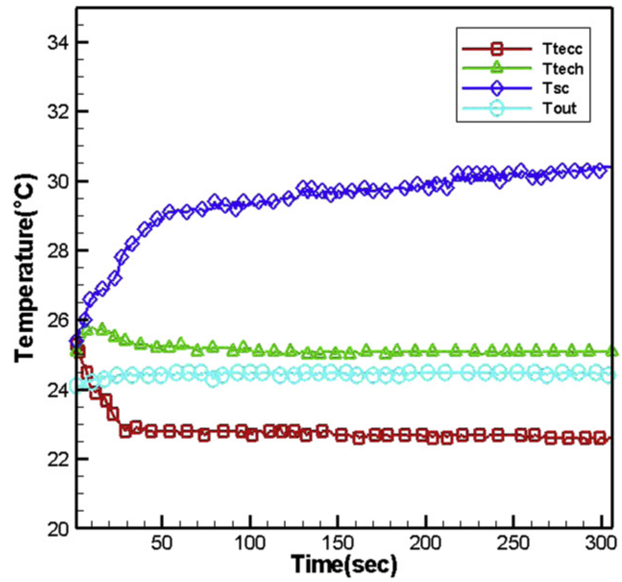

Fig. 3. Transient variation in the temperatures of solar cell, thermoelectric coolers and cooling water with water flow rate of 2500 ml/min.

temperature difference between their hot and the cold sides reaches around 10 °C in the same period. It is found that in the case without the cooling water the hot and the cold side temperatures exceed 44 °C and 34 °C, respectively. This implies that without the waste heat regeneration unit the module cannot be used to cool down the indoor space as an air conditioner.

When the cooling water is allowed to flow through the heat regeneration water channel, the performance of the combined module is greatly improved. Fig. 3 conveys transient variation in the temperatures of the solar cell, the hot and cold sides of the thermoelectric coolers and the exiting cooling water (T_{out}) at water flow rate of 2500 ml/min. It is clearly observed that the temperatures reach the steady-state regime after approximately 150 s furthermore, due to the cooling effects of the waste heat regeneration unit, the steady-state temperature of the solar cell is greatly reduced to 30.5 °C, and the steady-state temperatures at the hot and cold sides of the thermoelectric coolers are reduced to 25 °C and 22.5 °C, respectively. The temperature of the exiting cooling water is only slightly elevated to 24.5 °C. The cold side temperature of the TEC is lower than the exiting cooling water temperature by around 2 °C. This confirms the findings of the previous studies [9,20] that an increase in the convection heat transfer coefficient on the hot side of the thermoelectric coolers can remarkably reduce the temperature of the thermoelectric coolers. Note that the cooling effects can be further improved if more solar cells and TECs are in use. The water can also be circulated in a close loop for a period of time to increase its temperature before it is stored in the hot water tank; however, a higher temperature of the cooling water results in increases in the temperatures of the solar cells and the thermoelectric coolers.

As described by Wysocki and Rappaport [24] and Adawi and Nuaim [25], the temperature of the solar cell exhibits subtle influence on the junction current, recombination current and photovoltaic voltage of the solar cell. Since the solar cell temperature can be changed by adjusting the flow rate of the cooling water, it is essential to examine the dependence of the solar cell output power on the flow rate of the cooling water. As plotted in Fig. 4, the steady-state temperature of the solar cell is decreased by increasing the flow rate of the cooling water. As a result, the steady-state output power of the solar cell increases with the flow rate of the

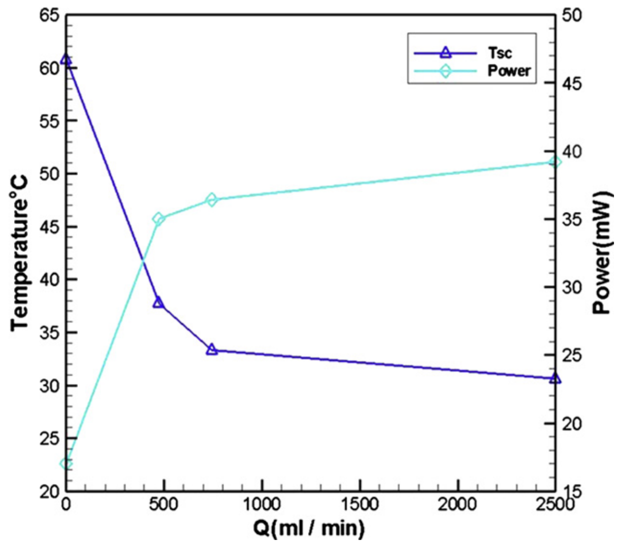

Fig. 4. Effects of cooling water flow rate on the steady-state temperature and output power of each solar cell.

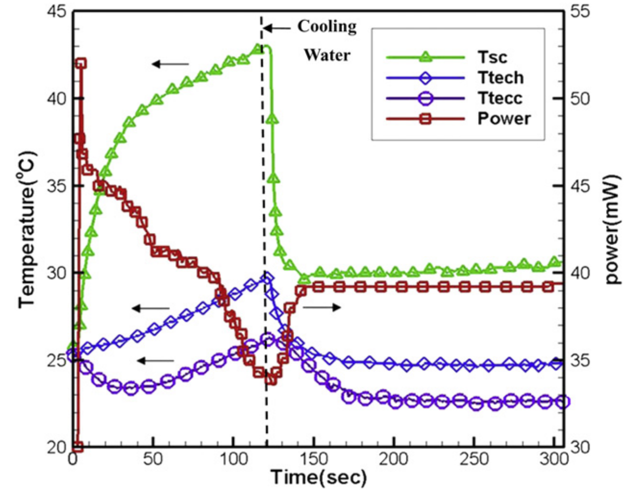

Fig. 6. Transient variation in output power of solar cell and temperatures of solar cell and thermoelectric coolers in flow interrupt test (before 120 s, flow rate = 0; after 120 s, flow rate = 2500 ml/min).

cooling water. The observation agrees with the findings of [23,24]. In addition, it is found that when the flow rate is 2500 ml/min, the steady-state temperature of the solar is reduced to 30.5 °C. However, at a flow rate of 750 ml/min, the solar cell temperature is still reduced to 33.2 °C. This implies that the flow rate of the cooling water may not exceed 750 ml/min as only for cooling purpose.

Fig. 5 shows the effects of cooling water flow rate on the steady-state temperatures of thermoelectric cooler and existing cooling water. Similarly, the steady-state temperatures of the thermoelectric cooler and the existing cooling water are decreased by increasing the flow rate of the cooling water. Again, at a flow rate over 750 ml/min, these temperatures are only reduced by just small values. In addition, it is noticed that as the cooling flow rate is elevated to a value over 2000 ml/min, the steady-state temperatures of the exiting cooling water and the hot side of the thermoelectric cooler are nearly of the same value (close to 24 °C). Also noted is that as the flow rate is higher than 2000 ml/min, the steady-state solar cell temperature is around 31 °C (as shown in Fig. 4) and that of the cold side of the thermoelectric cooler is around 22.5 °C. At the flow rate of 2500 ml/min, it seems that the temperature of the exiting cooling water is higher than that of the hot side temperature of the thermoelectric cooler. This probably may be attributed to the uncertainty of the temperature measurement.

The dependence of T_{tech}, T_{tecc} and T_{sc} and the output power of the solar cell can be more clearly observed based on the flow interrupt test results shown in Fig. 6. In the test, the combined module is operated without cooling water flowing through the heat regeneration channel in the first 120 s after start-up. The valve of cooling water flow is suddenly open at 120 s, and the cooling water is supplied at 2500 ml/min to the waste heat regeneration unit. As shown in Fig. 6, the magnitudes of T_{tech}, T_{tecc} and T_{sc} all increase, while the power of the solar cell decreases rapidly, with time in the first 120 s. Once the cooling water of 24 °C is supplied, all the temperatures of the combined module are rapidly reduced and the output power of the solar cell is greatly elevated from 33.5 to 39.5 mW in only 30 s.

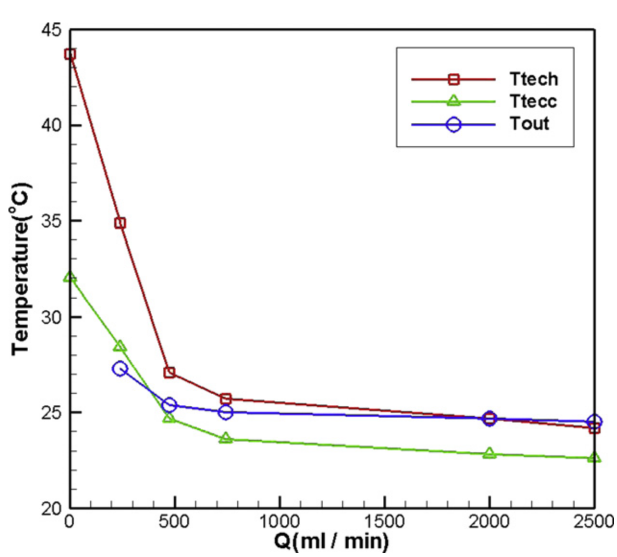

Fig. 5. Effects of cooling water flow rate on the temperatures of thermoelectric cooler and existing cooling water.

3.2. Applications of the combined module in the model house

Next, the design concept of the combined module with waste heat regeneration unit is tested in the applications in a model house. Fig. 7(a) shows the photograph of the model house and the data logger. The size of the model house is 30 cm × 12 cm × 10 cm, and the walls of the model house are made of wooden plates and the floor is made of Bakelite plates. For applications in the model house, two combined modules are made and the design of the combined module is slightly modified. Each of the two combined modules has one solar cells (12 V, 15 W) and two 30 mm × 30 mm thermoelectric coolers, and in between the solar cell and the thermoelectric coolers there is a cooling water channels, as described in the precedent sections. The two combined modules are used to build the symmetric ^-shape roof of the model house. These two solar cells used in the two combined modules are actually connected in series to drive the four thermoelectric coolers which are arranged in parallel. A power controller with a lithium battery is installed to control the input current of thermoelectric coolers from the solar cells. The cooling water is supplied by the constant-temperature bath and enters the channels at constant temperature (24 °C) and constant flow rate. During the

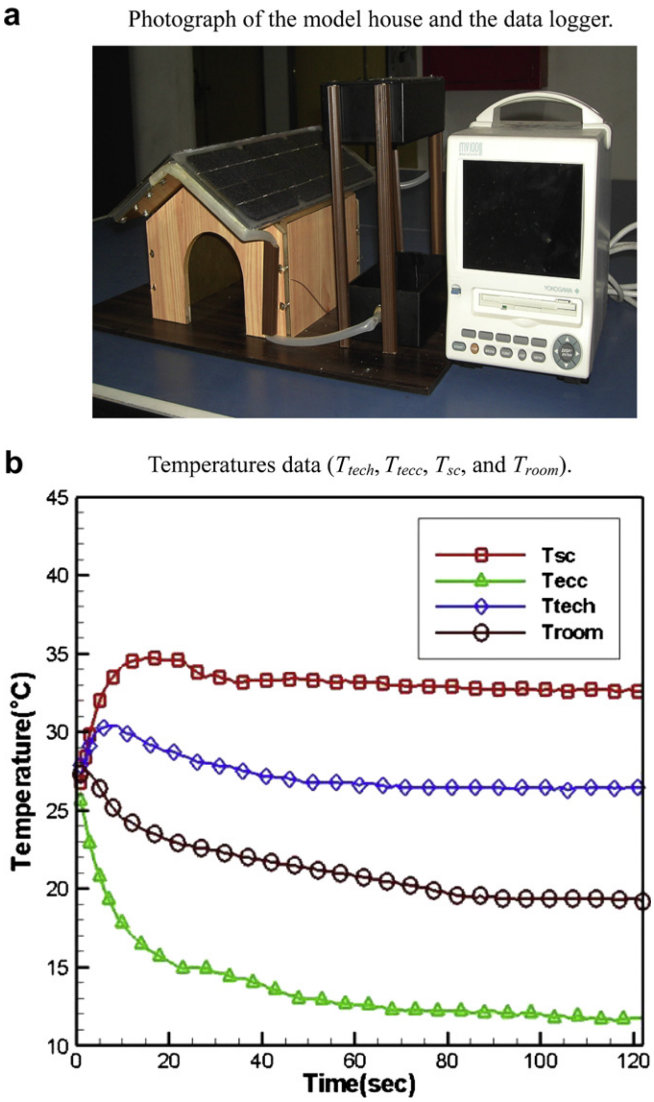

Fig. 7. Performance test of the combined modules used in model house, with 2000 ml/min cooling flow rate.

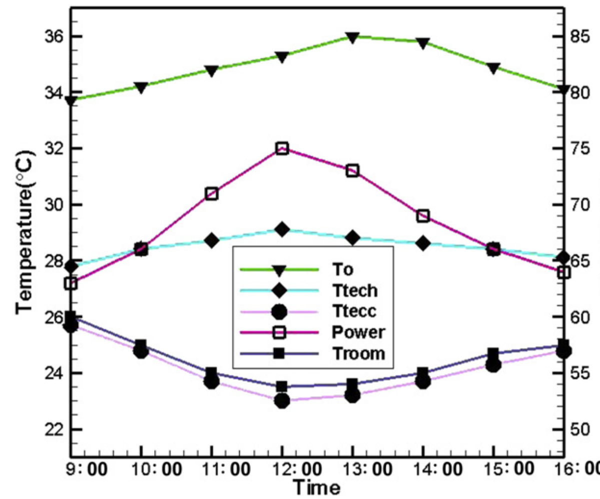

Fig. 8. Temperature variation of model house and power of solar cells roof at the cooling flow rate $Q = 2000$ ml/min under the real solar radiation condition. Experiments were performed on September 1, 2010 in Tainan City, Taiwan (120E12′00", 23N00′00").

experiments, the door and the windows of the model house is closed. The ambient temperature (T_∞) and the temperature of the air in the model house (T_{room}) are measured by using two T-type thermocouples. Measurement of the temperatures of the solar cells and the thermoelectric coolers are performed by exactly the same methods described earlier. The values of T_{tech}, T_{tecc} and T_{sc} are determined by averaging the values measured in the two combined modules.

Fig. 7(b) shows the transient variations in T_{tech}, T_{tecc}, T_{sc}, and T_{room} at 2000 ml/min cooling water flow rate and 1.2 A input current. After the 500-W halogen lamp is switched on, the solar cells can reach a steady-state temperature of 32.6 °C in 120 s. It is also found that the steady-state temperatures of the hot and the cold sides of the TECs are 26.5 and 19.5 °C, and the air temperature in the model house eventually reaches 19.5 °C. During the experiments, the ambient temperature is measured to be 35.7 °C. It means that the present approach is able to produce a 16.2 °C temperature difference between the ambient temperature and the air temperature in the model house (T_∞-T_{room} = 35.7−19.5 = 16.2 °C). The combined module is capable of cooling down the indoor air of the model house.

Moreover, the model house is placed under the real solar radiation condition to justify the validity of the experiments. The variations of temperature at $Q = 2000$ ml/min is investigated in a typical sunny day (September 1, 2010 in Tainan City, Taiwan, 120E12′00", 23N00′00") when the ambient temperature T_o is about 34.9 ± 1.1 °C. The results are provided in Fig. 8. In this figure, the solar radiation has been obviously increased from 9:00, reached to the maximum value at 12:00 and then decreased gradually till sunset at 17:00. As expected, the output power of the solar cell roof, which is used by the thermoelectric elements, reaches the maximum value at 12:00. In many previous studies [9,12,15], more applied power to the thermoelectric elements will cause more temperature different. Therefore, as shown in Fig. 8, the temperature different ($T_{tech} - T_{tecc}$) is largest and T_{room}(=23.4 °C) is lowest at 12:00 because of its largest solar radiation absorbed by the model house. Note that based on the experiments, it is found that the average intensity of solar energy is about 400–600 W/m^2 in the neighboring area of Kaohsiung city, Taiwan, in September. Therefore, the 500-W/m^2 halogen lamp is used to simulate a stable 500 W/m^2 solar radiation. The distance between the halogen lamp and the solar cell is fixed at 0.5 m because of the limitation of the vertex angle of the halogen lamp. However, in the real solar radiation experiment, the power of solar radiation strongly depends on time.

It is important to note that the evaluation of the impact of the cooling water temperature on the performance of system is really essential. Therefore, more experiments have been performed regarding the effects of the inlet cooling temperature, and the results are shown in a Fig. 9. Also, the data regarding the coefficient of performance (COP) of the thermoelectric cooler, which are measured by the technology developed by Huang et al. [25], are provided. The cases shown in this figures are measured at 2000 ml/min cooling water flow rate and 0.7 A input current. It is found that the temperature difference between the hot and the cold sides of the thermoelectric cooler ($\Delta T = T_{tech} - T_{tecc}$) increases with the inlet cooling water temperature. This is because a higher cooling water temperature helps increase the hot side temperature while the cold side temperature change is relatively small. Thus, the value of ΔT grows with the inlet cooling water temperature. Meanwhile, it is found that the magnitude of COP is decreased by increasing the inlet cooling water temperature. The

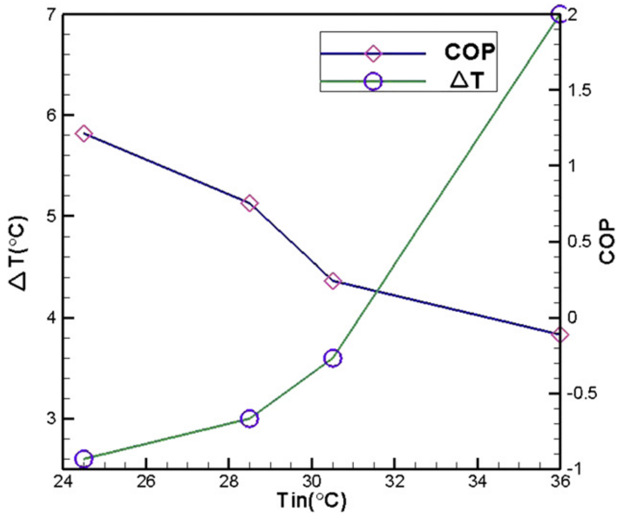

Fig. 9. Coefficient of performance (COP) and temperature difference between the hot and the cold sides of the TEC ($\Delta T = T_{tech} - T_{tecc}$) as a function if inlet cooling water temperature (T_{in}), at $Q = 2000$ ml/min and $I = 0.7$ A.

magnitude of COP is calculated by Q_c/W_{in}, where Q_c is the rate of heat absorbed by cold side of the thermoelectric cooler, which is determined from the difference between the ambient temperature and the cold side temperature, $T_o - T_{tecc}$. One may expect that an increase in T_{tecc} resulted from the elevation of T_{in} leads to a decrease in both Q_c and COP. Note that as the inlet cooling water temperature is increased to be 36 °C, the cold side temperature reaches a value higher than the ambient temperature. As a result, the values of Q_c and COP both become negative as shown in Fig. 9.

It is important to emphasize here that in this approach, the electricity consumed in the air-conditioning system of the model house is generated from the renewable energy by the solar cell installed the combined module itself. Furthermore the waste heat rejected by the solar cell and the thermoelectric cooler is utilized for water heating. Therefore, both the air-conditioning and the water heating demands can be satisfied without consuming any electricity provided from the external source. However, for a real green building whose length scale might be enormous, the area or number of the combined module may also be enlarged in proportion to the size required; therefore, the design will depend on individual cases and further study might be needed.

4. Concluding remarks

In this study a solar-driven thermoelectric cooling module with a waste heat regeneration unit is proposed and tested. The solar cells are used to provide the electricity for the thermoelectric cooler which is employed to absorb heat from the indoor space of the green building and then dissipated heat to the cooling water flowing in the regeneration channel. A model house with the combined module has been built for testing the feasibility of this approach, and the experimental results are provided. The conclusions reached in the present study are listed as follows:

1. Cooling the solar cell is an important factor to improve the performance of our energy-saving module because it can easily raise the output power of solar cell. It is found that the steady-state temperature of the solar cell is decreased by increasing the flow rate of the cooling water. For the particular case considered in this study, when the flow rate is 2500 ml/min, the steady-state temperature of the solar is reduced to 30.5 °C. However, the flow rate of the cooling water may not exceed 750 ml/min since at a flow rate of 750 ml/min, the solar cell temperature is still reduced to 33.2 °C.
2. It is observed that the heat dissipated from the hot side of the thermoelectric cooler can also be efficiently removed by the cooling water to elevate the performance of the thermoelectric cooler. It is found that in the case without the cooling water the hot and the cold side temperatures of the thermoelectric cooler may be higher than 44 °C and 34 °C, respectively. Nevertheless, when the cooling water is allowed to flow through the heat regeneration water channel, the steady-state temperatures at the hot and cold sides of the thermoelectric cooler are reduced to 25 °C and 22.5 °C, respectively.
3. Furthermore the waste heat rejected by the solar cell and the thermoelectric cooler is utilized for water heating. Therefore, both the air-conditioning and the water heating demands can be satisfied without consuming any electricity provided from the external source.
4. Based on the model house tests, it is found that the present approach is able to produce a 16.2 °C temperature difference between the ambient temperature and the air temperature in the model house. This implies that the combined module is capable of cooling down the indoor air of the model house.

Acknowledgement

Authors would like to thank the National Space Organization, Taiwan, ROC, for their financial support and help in experiments.

References

[1] Mousazadeh H, Keyhani A, Javadi A, Mobli H, Abrinia K, Sharifi A. A review of principle and sun-tracking methods for maximizing solar systems output. Renewable and Sustainable Energy Reviews 2009;13:1800–18.
[2] Myers DR. Solar radiation modeling and measurements for renewable energy applications: data and model quality. Energy 2005;30:1517–31.
[3] Radziemska E. Thermal performance of Si and GaAs based solar cells and modules: a review. Progress in Energy and Combustion Science 2003;29:407–24.
[4] Toivola M, Peltokorpi L, Halme J, Lund P. Regenerative effects by temperature variations in dye-sensitized solar cells. Solar Energy Materials & Solar Cells 2007;91:1733–42.
[5] Radziemska E. The effect of temperature on the power drop in crystalline silicon solar cells. Renewable Energy 2003;28:1–12.
[6] Sabounch AM. Effect of ambient temperature on the demanded energy of solar cells at different inclinations. Renewable Energy 1998;14:149–55.
[7] Hirata Y, Inasaka T, Tani T. Output variation of photovoltaic modules with environmental factors-II: seasonal variation. Solar Energy 1988;63:185–9.
[8] Hsiao YY, Chang WC, Chen SL. A mathematic model of thermoelectric module with applications on waste heat recovery from automobile engine. Energy 2010;35:1447–54.
[9] Cheng CH, Huang SY, Cheng TC. A three-dimensional theoretical model for predicting transient thermal behavior of thermoelectric coolers. International Journal of Heat and Mass Transfer 2010;53:2001–11.
[10] Yamanashi M. A new approach to optimum design in thermoelectric cooling system. Journal of Applied Physics 1996;80:5494–502.
[11] Kubo M, Shinoda M, Furuhata T, Kitagawa K. Optimization of the incision size and cold-end temperature of a thermoelectric device. Energy 2005;30:2156–70.
[12] Chein R, Huang G. Thermoelectric cooler application in electronic cooling. Applied Thermal Engineering 2004;24:2207–17.
[13] Mitrani D, Salazar J, Turo' A, Garcı' MA, Cha've JA. One-dimensional modeling of TE devices considering temperature-dependent parameters using SPICE. Microelectronics Journal 2009;40:1398–405.
[14] Xuan XC. Investigation of thermal contact effect on thermoelectric coolers. Energy Conversion and Management 2003;44:399–410.
[15] Lee KH, Kim OJ. Analysis on the cooling performance of the thermoelectric micro-cooler. International Journal of Heat and Mass Transfer 2007;50:1982–92.
[16] Hara T, Azuma H, Shimizu H, Obora H, Sato S. Cooling performance of solar cell driven, thermoelectric cooling prototype headgear. Applied Thermal Engineering 1998;18:1159–69.

[17] Mei VC, Chen FC, Mathiprakasam B, Heenan P. Study of solar-assisted thermoelectric technology for automobile air conditioning. Journal of Solar Energy Engineering Transactions of the ASME 1993;115:200–5.
[18] Bansal PK, Martin A. Comparative study of vapor compression, thermoelectric and absorption refrigerators. International Journal of Energy Research 2000; 24:93–107.
[19] Xi H, Luo L, Fraisse G. Development and applications of solar-based thermoelectric technologies. Renewable and Sustainable Energy Reviews 2007;11:923–36.
[20] Chein R, Chen Y. Performances of thermoelectric cooler integrated with microchannel heat sinks. International Journal of Refrigeration 2005;28: 828–39.
[21] Kline SJ, McClintock FA. Describing uncertainties in single-sample experiments. Mechanical Engineering 1953;75:3–8.
[22] Moffat RJ. Describing the uncertainties in experimental results. Experimental Thermal and Fluid Science 1988;1:3–17.
[23] Wysocki JJ, Rappaport P. Effect of temperature on photovoltaic solar energy conversion. Journal of Applied Physics 1960;31:571–8.
[24] Adawi MK, Nuaim IA. The temperature functional dependence of VOC for a solar cell in relation to its efficiency new approach. Desalination 2007;209: 91–6.
[25] Huang BJ, Chin CJ, Duang CL. A design method of thermoelectric cooler. International Journal of Refrigeration 2000;23:208–18.